Electrophoretic slip-tuned particle migration in microchannel viscoelastic fluid flows

Di Li and Xiangchun Xuan*
Department of Mechanical Engineering, Clemson University, Clemson, South Carolina 29634-0921, USA

(Received 15 January 2018; published 5 July 2018)

Particle migration is the underlying mechanism for continuous-flow focusing, trapping, and sorting of various types of particles in microfluidic devices. We present in this work an experimental investigation of the cross-stream migration of spherical polystyrene particles in a combined pressure- and electric field-driven flow of viscoelastic fluid through a straight rectangular microchannel. We find that particles migrate toward the centerline of the channel if they are leading the hydrodynamic flow due to positive electrophoresis. Conversely, lagging particles due to negative electrophoresis migrate toward the walls of the channel. These migrations are found to be exactly opposite to those in a Newtonian fluid in our control experiment. We attribute this phenomenon to the shear-induced extra lift in a viscoelastic fluid that has been recently predicted to arise from the nonlinear coupling of the electrophoretic particle motion with the local flow field. The effects of hydrodynamic flow rate and electric field magnitude on the bidirectional particle migrations are studied, which can both be reasonably explained using the theoretical formula of the electrophoretic motion-induced extra lift in a viscoelastic shear flow.

DOI: 10.1103/PhysRevFluids.3.074202

I. INTRODUCTION

Particle migration here refers to the cross-stream motion of particles in a flowing fluid through a confined channel. It enables the continuous focusing [1], trapping [2], and sorting [3,4] of various types of particles in microfluidic devices for a variety of applications. Particle migration can be driven by an externally imposed force (often categorized as an *active* method) ranging from the ubiquitous gravity [5] to acoustic [6], electric [7], magnetic [8], and optical [9] forces. It can also be generated by an internal flow-induced force (hence categorized as a *passive* method), including the inertial lift in Newtonian fluids [10,11] and the elastic/inertial lift in viscoelastic fluids [12–14]. Recently, there has been a growing interest in the integration of *active* and *passive* manipulations of particle migration in microchannels for enhanced specificity, throughput, accuracy and flexibility, etc. [15–17]. The earliest attempts in this direction may go to the studies of migration of nonneutrally buoyant particles in a vertical Couette or Poiseuille flow in 1960s [18–21]. Under such circumstances, the gravity (or buoyancy) effect generates a slip velocity between the particle and the suspending Newtonian fluid, which interacts with the local fluid shear yielding a so-called Saffman lift [22]. This lateral force can direct a flowing particle toward either the adjacent wall or the centerline of a channel depending on if the particle velocity is greater or less than the undisturbed fluid velocity [23–26]. It is unlike the wall-induced inertial lift that pushes particles away from any channel wall(s) or the shear gradient-induced inertial lift that pushes particles away from the channel centerline [27,28].

In a recent work, Kim and Yoo [29] proposed the use of a direct-current (DC) electric field to vary the particle velocity (in both the magnitude and direction) relative to a pressure-driven fluid flow

*xcxuan@clemson.edu

via electrophoresis. They demonstrated a three-dimensional focusing along the axis of a cylindrical capillary for both polystyrene microspheres [29] and red blood cells [30] that lag behind an inertialess water-glycerol flow due to negative electrophoresis. They also reported a similar particle focusing along the central axis of a rectangular microchannel [31]. Such an electrophoretic slip-induced particle migration was later extended by Yuan *et al.* [32] to modify the inertial focusing of polystyrene microspheres in a straight rectangular microchannel with symmetric obstacle arrays patterned on its sidewalls. They demonstrated that the inertial focusing position can be readily switched from along the channel center (for lagging particles) to toward the channel walls (for leading particles) by reversing the direction of the applied DC electric field. In addition, Cevheri and Yoda [33] observed the self-assembly of submicron polystyrene particles into streamwise bands within 1 μm of the wall in a countercurrent Poiseuille and electroosmotic flow of electrolyte solution. Such an interesting phenomenon may be associated with the wall-directed Saffman lift due to the positive electrophoretic slip. This correlation seems to be supported by the measured Saffman lift-like repulsion force in Cevheri and Yoda's paper [34], which pushes submicron particles away from the wall in a concurrent Poiseuille and electroosmotic flow (where particles experience negative electrophoresis and hence lag behind the fluid flow).

In another study, Zheng and Yeung [35] reported an anomalous radial migration of DNA molecules in capillary electrophoresis with an applied Poiseuille flow. They observed that λ-DNA molecules in a Gly-Gly buffer solution move toward the center (wall) of the capillary when the hydrodynamic flow is applied from the cathode (anode) to the anode (cathode). As their electrophoretic motion is from the cathode to the anode, DNA molecules migrate towards the capillary center and wall when they lead and lag the fluid flow, respectively. This is exactly opposite to the reported migrations of polystyrene particles [29,31–34] and biological cells [30] in Newtonian fluids as reviewed above. Zheng and Yeung [36] explained their experimental observations using the deformation of DNA molecules in a shear flow, which is size dependent and hence can be utilized to separate large molecules. Later, Ladd and his coworkers [37,38] developed a dumbbell kinetic theory to investigate the mechanism that causes the cross-stream migration of confined polymers under the influence of an external force parallel to the flow filed. They attributed the migration of DNA molecules to the asymmetric hydrodynamic interactions between polymer segments and the confining walls [39]. Recently, the same group [40] reported a systematic investigation of the parametric effects on the increase of DNA concentration in the center of a square microchannel when the flow and electric field drive the polymer in the same direction. They also demonstrated an electro-hydrodynamic concentration of genomic length DNA by the use of the outward polyelectrolyte migration with the near-wall electrophoretic recirculation [41].

We speculate that the opposite lateral migration of DNA molecules [35–41] to that of polystyrene particles [29–34] in a confined electrohydrodynamic flow of Newtonian fluids may be correlated with the viscoelastic property of the DNA solution itself. Note that the viscoelastic feature of DNA solutions has been extensively studied through both flow visualizations [42] and particle manipulations [43] in various microchannels. To verify our hypothesis, we provide in this work further experimental evidences via a direct comparison of the electrophoretic slip-tuned particle migration in the flow of a viscoelastic fluid and a Newtonian fluid, respectively, through a straight rectangular microchannel. We observe exactly opposite migrations in between the two fluids, which is attributed to the electrophoretic motion-induced extra lift in the viscoelastic fluid. Such a fluid elasticity-originated lift has been recently predicted to arise from the nonlinear coupling of an external force-driven particle motion (here, electrophoresis) and the local viscoelastic shear flow [44,45]. We also attempt to use this electrophoretic motion-induced extra lift to explain the observed flow rate and electric field effects on particle migration in the viscoelastic fluid flow.

II. EXPERIMENT

Figure 1 shows a picture of the microfluidic chip used in our experiment. The microchip was fabricated with polydimethylsiloxane (PDMS) using the standard soft lithography technique as

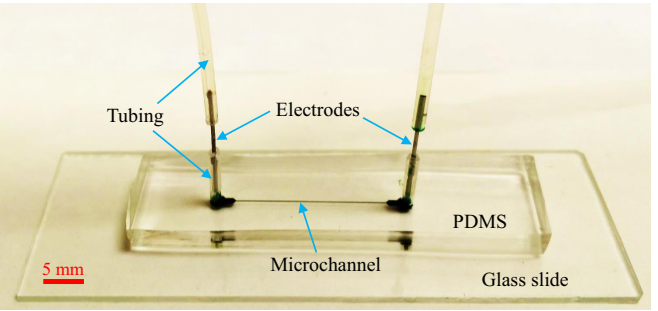

FIG. 1. Picture of the microfluidic chip used in experiment. The microchannel is filled with green food dye for clarity. The electrodes are shortened stainless steel needles with each end being inserted into a plastic tubing.

described elsewhere [46]. It is composed of a 3-mm-thick PDMS slab and a 1-mm-thick regular glass slide with a 2-cm-long straight rectangular microchannel sandwiched in between. The channel is 50 μm wide, 100 μm deep, and has an expansion region at either end that is each connected to a short polyethylene tubing (United States Plastic Corporation). An array of posts was designed at the channel expansion for blocking out any debris. A stainless-steel electrode (cut from a syringe needle, Fisher Scientific) was inserted into each of the short tubing on one end and connected to a long polyethylene tubing on the other end. One long tubing was connected with a high-precision infusion syringe pump (KD Scientific) for fluid actuation and the other long tubing was connected to an open container for fluid drainage. Electric field was supplied by a high-voltage DC power supply (Glassman High Voltage) via a wire connection to each of the stainless steel electrodes.

The particle solution was prepared by resuspending 10 μm diameter polystyrene spheres (Thermo Scientific) into either a non-Newtonian fluid or a Newtonian fluid (for a control experiment). Both suspending fluids were made of 0.01 mM phosphate buffer that was mixed with 0.5% (volume ratio) Tween 20 (Fisher Scientific) to minimize particle adhesions (to channel walls) and aggregations. The non-Newtonian fluid was prepared by dissolving polyethylene oxide (PEO, molecular weight $= 2\times10^6$g/mol, Sigma-Aldrich) powder into the buffer solution at a concentration of 1000 ppm. The particle concentration was kept low ($<0.1\%$ in volume fraction) in either fluid, and hence its effect on fluid viscosity can be neglected [47]. The microchannel was primed with the particle-free suspending fluid prior to the introduction of the particle suspension. Particle motion was visualized at both the inlet and outlet of the microchannel through an inverted microscope (Nikon Eclipse TE2000U) equipped with a CCD camera (Nikon DS-Qi1MC). Digital videos were recorded at a rate of around 15 frames per second, from which snapshot and superimposed images could be obtained and further processed (if needed) in the Nikon imaging software (NIS-Elements AR 3.22).

III. THEORY

We analyze in this section the field-induced forces that are pertinent to the particle migration in a combined pressure- and electric field-driven flow of viscoelastic fluid through a straight rectangular microchannel. The origin of the three-dimensional coordinates was set to the center of the channel inlet for convenience (Fig. 2). The following assumptions are made to simplify the analysis: (I) the electroosmotic flow is negligible because of the charge suppression effect of the neutral PEO polymer on microchannel walls [48]; (II) the hydrodynamic flow is fully developed in the microchannel with a uni-directional fluid velocity along the length direction, $\mathbf{V} = U(y,z)\mathbf{i}$, where $\mathbf{i}$ is the unit vector in the x direction; (III) fluid properties remain constant throughout the microchannel due to insignificant Joule heating effects (the estimated temperature rise, $\Delta T = \sigma E^2 D^2/k < 0.01$ K, where σ, E, D, and k are the fluid electric conductivity, electric field magnitude, channel hydraulic diameter, and fluid thermal conductivity, respectively) even for the highest electric field used in our experiment

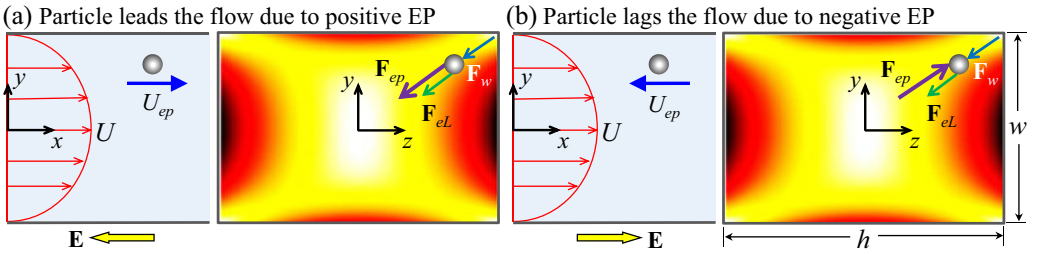

FIG. 2. Schematic illustration of electrophoretic slip, U_{ep}, tuned particle migration when a particle is leading (a) or lagging (b) a viscoelastic fluid flow, $U(y,z)$, in a straight rectangular microchannel (see the view in the x-y plane): the wall-induced electrical lift, $\mathbf{F}_w$, pushes the particle away from any walls; the flow-induced elastic lift, $\mathbf{F}_{eL}$, directs the particle towards the channel center (where the fluid shear rate is low as seen from the contour in the y-z plane, the darker color the larger magnitude) unless the particle is very close to any corners; the electrophoretic motion-induced extra lift, $\mathbf{F}_{ep}$, directs the leading particle away from the walls (a) and the lagging particle towards the walls (b) (see the view in the y-z plane). Note that the flow-induced viscous drag force, $\mathbf{F}_D$, in the y-z plane, which is opposite to the particle moving direction relative to the fluid, is not included on the plots. The origin of the coordinates is at the center of the channel inlet for convenience.

[49]; (IV) the effects of the wall and shear gradient-induced inertial lift forces [27,28] on particle migration are negligible because the calculated particle Reynolds number, Re_p, is smaller than 0.02 even under the largest flow rate in our experiment [50],

$$\mathrm{Re}_p = \mathrm{Re}\left(\frac{2a}{D}\right)^2, \tag{1}$$

$$\mathrm{Re} = \frac{\rho \bar{V} D}{\eta_0} = \frac{2\rho Q}{\eta_0 (w+h)}, \tag{2}$$

where Re is the (channel) Reynolds number, a is the particle radius, $\rho = 1.0\,\mathrm{g/cm^3}$ is the fluid density, $\bar{V}$ is the average fluid velocity, $\eta_0 = 2.3$ mPa·s is the zero-shear fluid viscosity [51], Q is the hydrodynamic flow rate, w and h are the channel width and height, respectively; (V) the gravity effect on particle migration is neglected considering the approximate matching of the particle and fluid densities.

A. Wall-induced electrical lift

The imposed DC electric field, $\mathbf{E}$, generates the traditional particle electrophoresis, $\mathbf{U}_{ep} = \mu_{ep}\mathbf{E}$, along the length direction of a straight rectangular microchannel, where μ_{ep} is the electrophoretic mobility. The electric field also exerts an electrical force on an off-center particle that pushes it away from any channel walls (Fig. 2) [52]. This wall-induced dielectrophoretic-like lift force, $\mathbf{F}_w$, arises from the asymmetric electric field around the particle due to its unmatched electric conductivity with the suspending fluid [53]. It can be considered using the formula recently proposed by Yariv [54] for a remote particle of radius a adjacent to a planar dielectric wall,

$$\mathbf{F}_w = f\varepsilon a^2 E^2 \mathbf{n}, \tag{3}$$

where f is a dimensionless coefficient that depends on the particle-fluid-channel system (e.g., particle blockage ratio and fluid ionic concentration, etc.) [55], ε is the fluid permittivity, and $\mathbf{n}$ is the unit vector normal to the wall pointing into the fluid. The electrical lift, $\mathbf{F}_w$, decays quickly for a particle moving away from a wall and becomes zero when the particle migrates to the centerline of a straight rectangular microchannel.

B. Flow-induced elastic lift

The non-uniform first normal stress difference, N_1, in a viscoelastic fluid flow generates a lift force that directs a particle suspended therein towards the low shear rate region [56], i.e., the channel centerline and corners (see the contour of fluid shear rate in the y-z plane in Fig. 2). This flow-induced elastic lift, $\mathbf{F}_{\mathrm{eL}}$, scales with the particle volume and can be estimated using the following formula [57],

$$\mathbf{F}_{\mathrm{eL}} = C_{\mathrm{eL}} a^3 \nabla N_1, \tag{4}$$

where C_{eL} is a non-dimensional elastic lift coefficient. Since the dilute PEO solution used in our experiment is a weakly shearing thinning fluid [58], we can use the Oldroyd-B model as a constitutive equation to evaluate N_1 [59], i.e.,

$$N_1 = 2\lambda \eta_p \dot{\gamma}^2, \tag{5}$$

where λ is the fluid relaxation time, η_p is the contribution of the PEO polymer to the fluid viscosity, and $\dot{\gamma}$ is the fluid shear rate. Thus, Eq. (4) can be rewritten as

$$\mathbf{F}_{\mathrm{eL}} = 2C_{\mathrm{eL}} a^3 \lambda \eta_p \nabla \dot{\gamma}^2, \tag{6}$$

For a fully developed flow in a straight rectangular microchannel (see Fig. 2), we have $\dot{\gamma}^2 = (\partial U/\partial y)^2 + (\partial U/\partial z)^2$. The magnitude of $\mathbf{F}_{\mathrm{eL}}$ increases with the Weissenberg number, Wi, that can be estimated using the following expression,

$$\mathrm{Wi} = \lambda \dot{\gamma} = \lambda \frac{2\bar{V}}{w} = \frac{2\lambda Q}{w^2 h}. \tag{7}$$

C. Electrophoretic motion-induced extra lift

The nonlinear coupling of an external force-driven particle motion with the local viscoelastic shear flow has been predicted in a couple of recent theoretical studies [44,45] to produce a lateral drift in a direction perpendicular to that force. We use the formula obtained by Einarsson and Mehlig [45] [see Eq. (62) therein] in an unbounded viscoelastic shear flow with the Oldroyd-B model to estimate the electrophoretic motion-induced extra lift, $\mathbf{F}_{\mathrm{ep}}$, in our experiment, which, to the first order of Wi, is written as

$$\mathbf{F}_{\mathrm{ep}} = -C_{\mathrm{ep}} W i \eta_r \Omega' \times (6\pi \eta_0 a \mathbf{U}_{\mathrm{ep}}), \tag{8}$$

where C_{ep} is a dimensionless coefficient that we introduce here to account for the particle confinement effects, $\eta_r = \eta_p/\eta_0$ is the relative contribution of elastic polymers to the total fluid viscosity, $\Omega' = \Omega/\dot{\gamma}$ is half the flow vorticity, $\Omega = \frac{1}{2}\nabla \times \mathbf{V}$, nondimensionalized by the shear rate. The whole term in the brackets on the right hand side of Eq. (8) can be viewed as the electric force that drives the electrophoretic particle motion [60]. Recognizing that $\mathbf{V} = U(y,z)\mathbf{i}$ for a fully developed flow in a straight rectangular microchannel, we have

$$\Omega = \frac{1}{2}\left(\frac{\partial U}{\partial z}\mathbf{j} - \frac{\partial U}{\partial y}\mathbf{k}\right), \tag{9}$$

$$\Omega \times \mathbf{U}_{\mathrm{ep}} = -\frac{1}{2}\left(\frac{\partial U}{\partial y}\mathbf{j} + \frac{\partial U}{\partial z}\mathbf{k}\right) U_{\mathrm{ep}}, \tag{10}$$

where $\mathbf{j}$ and $\mathbf{k}$ are the unit vectors in the y and z directions, respectively. Thus, Eq. (8) can be rewritten as

$$\mathbf{F}_{\mathrm{ep}} = C_{\mathrm{ep}}(3\pi \eta_p a)\lambda \left(\frac{\partial U}{\partial y}\mathbf{j} + \frac{\partial U}{\partial z}\mathbf{k}\right) U_{\mathrm{ep}}. \tag{11}$$

Therefore, the electrophoretic motion-induced extra lift in a viscoelastic fluid, $\mathbf{F}_{ep}$ (<0, due to the negative values of $\partial U/\partial y$ and $\partial U/\partial z$ in the first quadrant), directs a particle towards the channel centerline (i.e., $y = z = 0$,) when the particle leads the flow with a positive U_{ep} in Fig. 2(a). On the contrary, $\mathbf{F}_{ep}$ (>0) directs a particle away from the channel centerline when the particle lags the flow with a negative U_{ep} in Fig. 2(b). Moreover, $\mathbf{F}_{ep}$ scales linearly with the electrophoretic particle motion and hydrodynamic flow rate as well as the particle size. It becomes zero at the channel centerline due to the local zero shear rate and gets larger for particles nearer to any channel walls.

D. Flow-induced drag

The three lift forces presented above act together causing a cross-stream migration of a particle, which is balanced by a viscous drag, $\mathbf{F}_D$. Due to the very small particle Reynolds number in our experiment, we assume the particle experiences Stokes' drag,

$$\mathbf{F}_D = -6\pi\eta_0 a K \mathbf{U}_{p\_tr}, \tag{12}$$

where K is the correction factor for the wall retardation effects on particle motion in confined flows [61], and $\mathbf{U}_{p\_tr}$ is the particle migration velocity in the transverse direction (i.e., the y-z plane in Fig. 2). The streamwise particle travelling velocity, U_{p_st}, in the channel length direction (i.e., the x direction in Fig. 2) is equal to the summation of the local fluid velocity and the particle electrophoretic velocity (which can be either positive or negative depending on the direction of the applied electric field),

$$U_{p\_st} = U(y,z) + U_{ep}. \tag{13}$$

The particle migration velocity, $\mathbf{U}_{p\_tr}$, over the channel cross-section can be obtained from the quasi-steady balance of the above-presented lift and drag forces acting on a particle under a small Stokes number, i.e.,

$$\mathbf{U}_{p\_tr} = \frac{\mathbf{F}_w + \mathbf{F}_{eL} + \mathbf{F}_{ep}}{6\pi\eta_0 a K}. \tag{14}$$

IV. RESULTS AND DISCUSSION

A. Electrophoretic slip-tuned particle migration

Figure 3 shows the experimentally obtained images of electrophoretic slip-tuned 10-μm particle migration in the flow of PEO solution through a straight rectangular microchannel. In the absence of electric field, particles travel along with the viscoelastic fluid flow with zero electrophoretic slip. No apparent cross-stream particle migration is viewed from the image at the channel outlet in Fig. 3(b), which indicates an insignificant elastic focusing effect (the estimated Weissenberg number is Wi = 0.44 if the fluid relaxation time is assumed to be $\lambda = 1.5$ ms [62]). Under a negative 300 V/cm DC electric field (see Fig. 2), particles lead the viscoelastic fluid flow with a positive electrophoretic slip and migrate toward the centerline at the channel outlet in Fig. 3(a). On the contrary, particles migrate towards the channel walls at the outlet in Fig. 3(c) when they lag the viscoelastic fluid flow with a negative electrophoretic slip. This latter observation seems to be consistent with a recent experiment from Ranchon *et al.* [63], who demonstrated the migration of submicron polystyrene particles toward the channel walls in a hydrodynamic flow of viscoelastic polyvinylpyrrolidone (PVP) solution with a counter electrophoretic actuation. As neither the electrical lift nor the elastic lift varies with the electric field direction, the reverse of the particle migration should arise from the electrophoretic motion-induced extra lift as a result of the directional switch of particle electrophoresis. It is important to point out that the role of the electrical lift is actually very weak in our experiment because the images in Fig. 3(d) indicate a negligible particle focusing effect in a purely electrokinetic flow. Moreover, neither the upstream contraction nor the downstream expansion (1 mm long each) is found to have a significant effect on particle migration inside the 2-cm-long straight microchannel, which is evidenced from the particle trajectories at either junction for every case in Fig. 3.

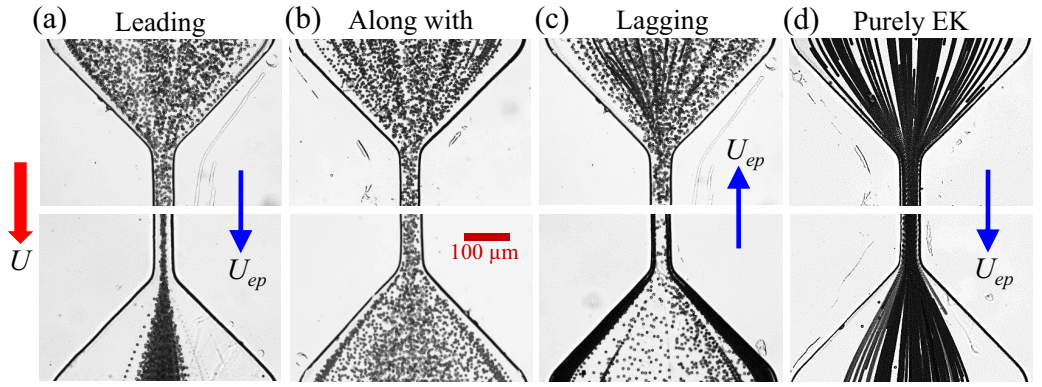

FIG. 3. Superimposed images of electrophoretic slip (U_{ep})-tuned migration for 10-μm-diameter particles leading (a, positive U_{ep}), along with (b, zero U_{ep}), and lagging (c, negative U_{ep}) the hydrodynamic flow of viscoelastic PEO solution (U, positive) at the channel inlet (top row) and outlet (bottom row), respectively. The pressure-driven flow rate is fixed at 125 μl/h, and the DC electric field is 300 V/cm for both the leading (a, negative direction) and lagging (c, positive direction) particles. Panel (d) shows the images of particle motion in a purely electrokinetic flow (i.e., in the absence of any pressure-driven flow).

The hydrodynamic flow rate in all the tests of Figs. 3(a)–3(c) was fixed at 125 μl/h, corresponding to an average fluid velocity, $V = 6.9$ mm/s, and a Reynolds number, $\mathrm{Re} = 0.21$ (at which $\mathrm{Re}_p = 0.005$). The magnitude of electrophoretic velocity for both the leading and lagging particles, $U_{ep} = 0.36$ mm/s, was calculated from the electrophoretic mobility, $\mu_{ep} = 1.2\times10^{-8}$ m^2/(V • s), which was determined experimentally by tracking single particle motions in a pure electric field-driven flow [55]. Interestingly, the observed phenomena in Fig. 3 are exactly opposite to the electrophoretic slip-tuned particle migration in the flow of a Newtonian buffer solution through the same microchannel. As viewed from the images in Fig. 4, particles migrate towards the channel walls [Fig. 4(a)] or centerline [Fig. 4(c)] when they lead or lag the 25 μl/h Newtonian fluid flow due to a positive or negative electrophoretic slip under a 300 V/cm electric field. They again exhibit an invisible migration in a purely hydrodynamic flow of Newtonian fluid [Fig. 4(b)], similar to the observation in a purely hydrodynamic flow of viscoelastic fluid [Fig. 3(b)]. As the elastic lift force does not vary with electric

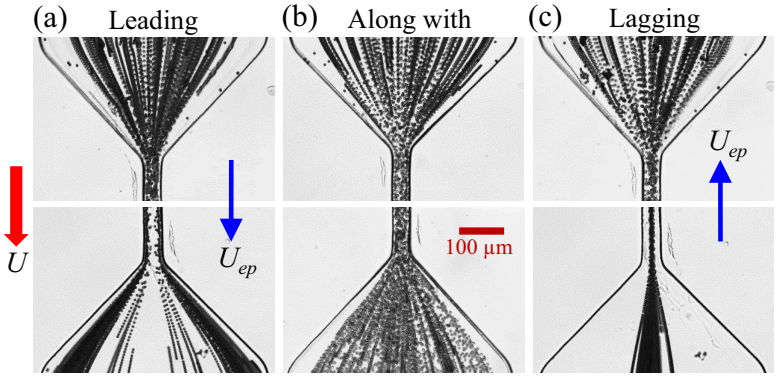

FIG. 4. Superimposed images of electrophoretic slip (U_{ep})-tuned migration for 10 μm-diameter particles leading (a, positive U_{ep}), along with (b, zero U_{ep}), and lagging (c, negative U_{ep}) the flow of Newtonian buffer solution (U, positive) at the channel inlet (top row) and outlet (bottom row), respectively. The hydrodynamic flow rate is fixed at 25 μl/h (as compared to 125 μl/h viscoelastic fluid flow in Fig. 3), and the DC electric field is 300 V/cm in both (a) (negative direction) and (c) (positive direction).

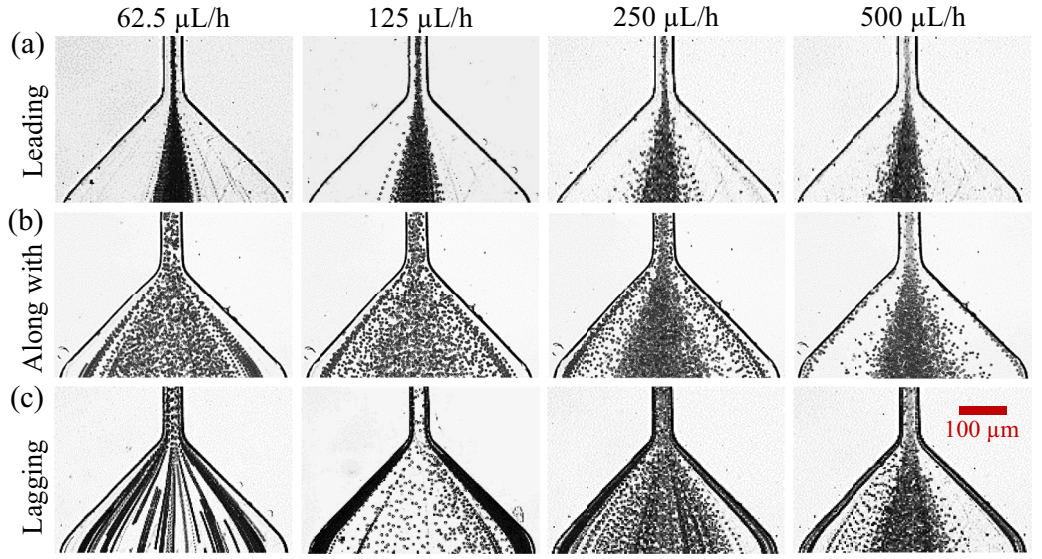

FIG. 5. Superimposed images of electrophoretic slip-tuned migration for 10-μm-diameter particles leading (a), along with (b), and lagging (c) the flow of 1000 ppm PEO solution at the channel outlet under various flow rates. Particles move from top to bottom in all images. The DC electric field is 300 V/cm for both the leading (positive downward direction) and lagging (negative upward direction) particles.

field direction, we attribute the opposite particle migrations in the viscoelastic buffer solution to the electrophoretic motion-induced extra lift therein. It is important to note that the hydrodynamic flow rate of the Newtonian fluid, at which the particle migrations are observed in Fig. 4, is much smaller than that of the viscoelastic fluid in Fig. 3. This may imply that the electrophoretic motion-induced extra lift in a viscoelastic fluid is significantly stronger than the traditional Saffman lift in a Newtonian fluid.

B. Effect of hydrodynamic flow rate

Figure 5 shows the effect of flow rate on electrophoretic slip-tuned migration of 10-μm particles in the hydrodynamic flow of 1000 ppm PEO solution through a straight rectangular microchannel. The DC electric field magnitude is 300 V/cm for both the leading (positive direction) and lagging (negative direction) particles. In the absence of electric field, particles experience zero electrophoretic slip and exhibit an apparently enhanced elastic focusing towards the channel center region at higher flow rates [Fig. 5(b)]. This is reflected by the increasing value of Weissenberg number, Wi, from 0.22 to 1.75 in the range of flow rates from 62.5 μl/h to 500 μl/h. The inertial focusing effect is estimated weak as the largest Reynolds number is still less than 1. In contrast, the leading particles are well focused to the channel centerline even at the smallest flow rate due to the additional action of the electrophoretic motion-induced extra lift [Fig. 5(a)]. However, such an electrophoresis-enhanced elastic focusing gets slightly worse with the increase of flow rate. In addition, Fig. 5(c) demonstrates that the lagging particles migrate towards the channel walls when the flow rate is increased from 62. 5 μl/h to 125 μl/h. This migration is also weakened at higher flow rates due to the increasing while opposing role of the elastic lift [Fig. 5(b)], where more particles migrate towards the channel centerline than those towards the walls. Interestingly, the migration of lagging particles at 500 μl/h becomes visually close to that of particles along with the fluid flow in Fig. 5(b).

Figure 6 shows the quantitative comparison of the experimentally measured stream widths for particles ahead of and along with the viscoelastic fluid flow. While the leading particles are much better focused in the range of the flow rates under test, we anticipate that the two types of focusing

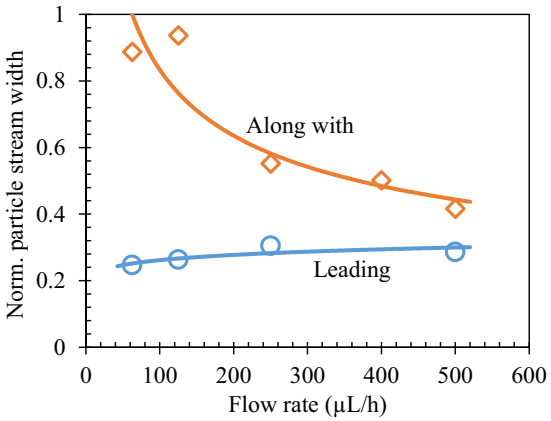

FIG. 6. Comparison of electrophoresis-enhanced elastic focusing (for leading particles with a positive electrophoretic slip) with purely elastic focusing (for particles traveling along with the fluid with zero electrophoretic slip) of 10-μm particles in the flow of 1000 ppm PEO solution through a straight rectangular microchannel. The symbols represent the measured values of the focused particle stream width (normalized by the channel width) from the images in Fig. 5. The curves are each the power trendline of the experimental data points.

effects will become similar with the further increase of flow rate due to the increasingly dominant elastic lift (and as well the inertial lift), $\mathbf{F}_{eL}$, over the electrophoretic motion-induced extra lift, $\mathbf{F}_{ep}$. This can be understood from the dissimilar dependences of $\mathbf{F}_{eL}$ and $\mathbf{F}_{ep}$ on the fluid shear rate. Specifically, as the contribution of the electrical lift, $\mathbf{F}_{w}$, is weak in our experiment [see Fig. 3(d)],

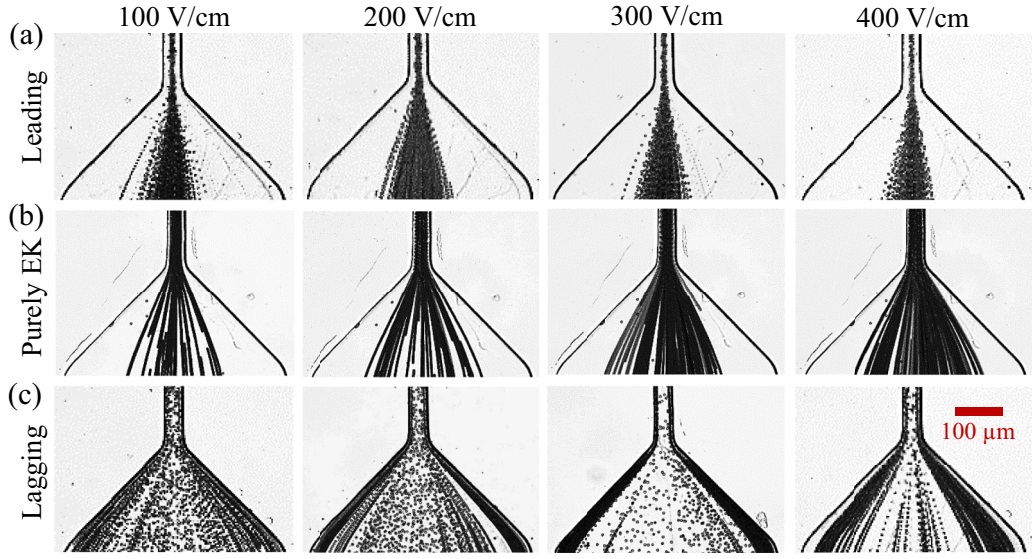

FIG. 7. Superimposed images of electrophoretic slip-tuned migration for 10-μm-diameter particles leading (a) and lagging (c) the flow of 1000 ppm PEO solution at the channel outlet under various DC electric fields. The hydrodynamic flow rate is fixed at 125 μl/h. (b) shows the images of particle motion in purely electrokinetic flows (i.e., in the absence of the pressure-driven flow) under the same DC electric fields as in panels (a) and (c). Particles move from top to bottom in all images.

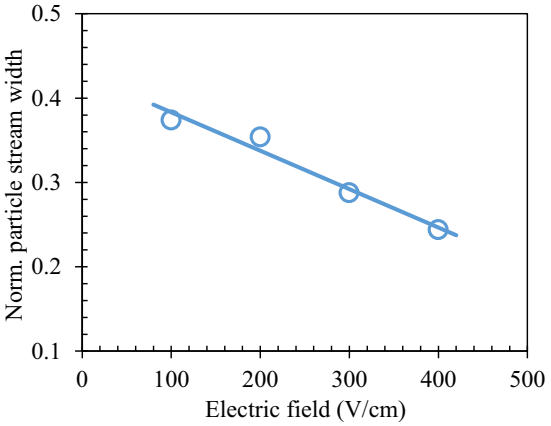

FIG. 8. Electric field effect on electrophoresis-enhanced elastic focusing of 10-μm particles leading the flow of 1000 ppm PEO solution in a straight rectangular microchannel. The symbols represent the measured values of the focused particle stream width (normalized by the channel width) from the images in Fig. 7. The curve is a linear trendline of the experimental data points.

the transverse particle migration velocity, $\mathbf{U}_{\text{p\_tr}}$, in Eq. (14) is reduced to

$$\mathbf{U}_{\text{p\_tr}} \cong \frac{C_{\text{eL}} a^2 \lambda \eta_r}{3\pi K} \nabla \dot{\gamma}^2 + \frac{C_{\text{ep}} \lambda \eta_r}{2K} \left(\frac{\partial U}{\partial y}\mathbf{j} + \frac{\partial U}{\partial z}\mathbf{k} \right) U_{\text{ep}}. \tag{15}$$

Further considering the much smaller magnitude of electrophoretic particle velocity as compared to that of the hydrodynamic fluid velocity, we simplify the streamwise particle travelling velocity as $U_{\text{p\_st}} \cong U(y,z)$. The lateral particle migration distance (and in turn the particle focusing) is dependent on the ratio of the cross-stream and streamwise particle speeds, which, for a fully-developed flow in a straight rectangular microchannel, is written as

$$\frac{\mathbf{U}_{\text{p\_tr}}}{U_{\text{p\_st}}} \cong \frac{C_{\text{eL}} a^2 \lambda \eta_r}{3\pi K} \frac{\nabla\left[\left(\frac{\partial U}{\partial y}\right)^2 + \left(\frac{\partial U}{\partial z}\right)^2\right]}{U(y,z)} + \frac{C_{\text{ep}} \lambda \eta_r}{2K} \frac{\left(\frac{\partial U}{\partial y}\mathbf{j} + \frac{\partial U}{\partial z}\mathbf{k}\right)}{U(y,z)} \mu_{\text{ep}} E. \tag{16}$$

Therefore, the elastic lift-induced particle migration (i.e., first term on the right-hand side) should increase with the flow rate in principle, which is consistent with the curve of decreasing particle stream width for particles along with the flow in Fig. 6. It is, however, important to note that this viscoelastic migration is not simply a linear function of the flow rate because of the position dependence of the flow velocity, $U(y,z)$, in a dynamic process. In contrast, the particle migration due to the electrophoretic motion-induced extra lift (i.e., second term on the right-hand side) is only a weak function of the flow rate, which explains why the stream width of leading particles in Fig. 6 does not change significantly with the flow rate when the elastic focusing effect is not sufficiently strong.

C. Effect of electric field

Figure 7 shows the effect of electric field magnitude on electrophoretic slip-tuned migration of 10-μm particles in the flow of 1000 ppm PEO solution through a straight rectangular microchannel. The hydrodynamic flow rate is fixed at 125 μl/h. With the increase of electric field from 100 to 400 V/cm, the leading particles achieve a better electrophoresis-enhanced elastic focusing in the viscoelastic fluid flow [Fig. 7(a)]. This enhancement does not come from the electrical lift-induced particle focusing as the latter effect in a purely electrokinetic flow was found very weak in the entire range of electric fields [Fig. 7(b)]. Surprisingly, such an electrokinetic particle focusing actually decreases at higher electric fields, which is inconsistent with both the prediction of Eq. (3) and our earlier studies [53,55,64]. The reason behind this phenomenon is currently unknown, but should be associated with the viscoelastic property of the suspending fluid. As the elastic lift is fixed regardless

of the electric field magnitude, the enhanced focusing of the leading particles should arise from the increased electrophoretic motion-induced extra lift. Moreover, as this shear-induced extra lift is proportional to the electrophoretic particle velocity, the resulting particle focusing effect at a fixed hydrodynamic flow rate increases linearly with the electric field magnitude as viewed from the second term on the right-hand side of Eq. (16). This is consistent with the linear trendline of the experimentally measured particle stream width in Fig. 8. Similarly, as viewed from the images in Fig. 7(c), the migration of lagging particles towards the channel walls also gets enhanced at higher electric fields because of the increasing wall-directed extra lift.

V. CONCLUSIONS

We have conducted a systematic experimental study of the cross-stream migration of particles in a combined pressure- and electric field-driven flow of viscoelastic and Newtonian fluids through a straight rectangular microchannel. We find that particles migrate towards the centerline or walls of the channel in a viscoelastic fluid when they are leading or lagging the flow due to electrophoresis. This migration is opposite to that in a Newtonian fluid, which may be a result of the fluid elasticity-induced extra lift due to the nonlinear coupling of the electrophoretic particle motion with the local shear flow. We also find that increasing the hydrodynamic flow rate reduces the particle migration of either direction in the viscoelastic fluid. This can be explained by the weaker dependence of the electrophoretic motion-induced extra lift on the shear rate than that of the elastic lift. In contrast, increasing the electric field enhances the particle migration of either direction due to the increased magnitude of the extra lift. In future work we will study how the fluid rheology (e.g., shear-thinning or shear-thickening) may affect the electrophoretic slip-tuned particle migration.

ACKNOWLEDGMENTS

This work was partially supported by NSF under Grant No. CBET-1704379 (X. Xuan). The authors thank Prof. Eric S. G. Shaqfeh for directing their attention to a couple of recent theoretical studies on the lateral drift of sedimenting particles in non-Newtonian fluid flows.

[1] X. Xuan, J. Zhu, and C. Church, Particle focusing in microfluidic devices, Microfluid. Nanofluid. **9**, 1 (2010).
[2] J. Nilsson, M. Evander, B. Hammarstrom, and T. Laurell, Review of cell and particle trapping in microfluidic systems, Anal. Chimica Acta **649**, 141 (2009).
[3] A. Karimi, S. Yazdi, and A. M. Ardekani, Hydrodynamic mechanisms of cell and particle trapping in microfluidics, Biomicrofluid. **7**, 021501 (2013).
[4] P. Sajeesh and A. K. Sen, Particle separation and sorting in microfluidic devices: a review, Microfluid. Nanofluid. **17**, 1 (2014).
[5] J. Song, M. Song, T. Kang, D. Kim, and L. P. Lee, Label-free density difference amplification-based cell sorting, Biomicrofluid. **8**, 064108 (2014).
[6] L. Y. Yeo and J. R. Friend, Surface acoustic wave microfluidics, Annu. Rev. Fluid Mech. **46**, 379 (2011).
[7] J. Regtmeier, R. Eichhorn, M. Viefhues, L. Bogunovic, and D. Anselmetti, Electrodeless dielectrophoresis for bioanalysis: Theory, devices and applications, Electrophor. **32**, 2253 (2011).
[8] M. Hejazian, W. Li, and N. T. Nguyen, Lab on a chip for continuous-flow magnetic cell separation, Lab Chip **15**, 959 (2015).
[9] A. A. Kayani, K. Khoshmanesh, S. A. Ward, A. Mitchell, and K. Kalantar-Zadeh, Optofluidics incorporating actively controlled micro-and nano-particles, Biomicrofluid. **6**, 031501 (2012).
[10] H. Amini, W. Lee, and D. Di Carlo, Inertial microfluidic physics, Lab Chip **14**, 2739 (2014).
[11] J. Zhang, S. Yan, D. Yuan, G. Alici, N. T. Nguyen, M. E. Warkiani, and W. Li, Fundamentals and applications of inertial microfluidics: a review, Lab Chip **16**, 10 (2016).

[12] G. D'Avino and P. L. Maffettone, Particle dynamics in viscoelastic liquids, J. Non-Newton. Fluid Mech. **215**, 80 (2015).
[13] G. D'Avino, F. Greco, and P. L. Maffettone, Particle migration due to viscoelasticity of the suspending liquid and its relevance in microfluidic devices, Annu. Rev. Fluid Mech. **49**, 341 (2017).
[14] X. Lu, C. Liu, G. Hu, and X. Xuan, Particle manipulations in non-Newtonian microfluidics: A review, J. Colloid Interface Sci. **500**, 182 (2017).
[15] Y. C. Kung, K. W. Huang, W. Chong, and P. Y. Chiou, Tunnel dielectrophoresis for tunable, single-stream cell focusing in physiological buffers in high-speed microfluidic flows, Small **12**, 4343 (2016).
[16] S. Yan, J. Zhang, D. Yuan, and W. Li, Hybrid microfluidics combined with active and passive approaches for continuous cell separation, Electrophor. **38**, 238 (2017).
[17] Y. Zhou, L. Song, L. Yu, and X. Xuan, Inertially focused diamagnetic particle separation in ferrofluids, Microfluid. Nanofluid. **21**, 14 (2017).
[18] D. R. Oliver, Influence of particle rotation on radial migration in the Poiseuille flow of suspensions, Nature **194**, 1269 (1962).
[19] R. V. Repetti and E. F. Leonard, Segre-Silberberg annulus formation: a possible explanation, Nature **203**, 1346 (1964).
[20] R. C. Jeffrey and J. R. A. Pearson, Particle motion in laminar vertical tube flow, J. Fluid Mech. **22**, 721 (1965).
[21] A. Karnis, H. L. Goldsmith, and S. G. Mason, The flow of suspensions through tubes. Part5: Inertial effects, Can. J. Chem. Eng. **44**, 181 (1966).
[22] P. G. Saffman, The lift on a small sphere in a slow shear flow, J. Fluid Mech. **22**, 385 (1965).
[23] J. S. Halow and G. B. Wills, Experimental observations of sphere migration in Couette systems, Indust. Eng. Chem. Fundam. **9**, 603 (1970).
[24] H. Aoki, Y. Kurosaki, and H. Anzai, Study on the tubular pinch effect in a pipe flow. I. Lateral migration of a single particle in laminar Poiseuille flow, Bull. JSME **22**, 206 (1979).
[25] A. J. Hogg, The inertial migration of non-neutrally buoyant spherical particles in two-dimensional shear flows, J. Fluid Mech. **272**, 285 (1994).
[26] J. Feng, H. H. Hu, and D. D. Joseph, Direct simulation of initial value problems for the motion of solid bodies in a Newtonian fluid. Part 2. Couette and Poiseuille flows, J. Fluid Mech. **277**, 271 (1994).
[27] B. P. Ho and L. G. Leal, Inertial migration of rigid spheres in two-dimensional unidirectional flows, J. Fluid Mech. **65**, 365 (1974).
[28] L. G. Leal, Particle motions in a viscous fluid, Annu. Rev. Fluid Mech. **12**, 435 (1980).
[29] Y. W. Kim and J. Y. Yoo, Axisymmetric flow focusing of particles in a single microchannel, Lab Chip **9**, 1043 (2009).
[30] Y. W. Kim and J. Y. Yoo, Three-dimensional focusing of red blood cells in microchannel flows for biosensing applications, Biosens. Bioelectron. **24**, 3677 (2009).
[31] Y. M. Kim and J. Y. Yoo, Bidirectional inward migration of particles lagging behind a Poiseuille flow in a rectangular microchannel for 3D particle focusing, J. Micromech. Microeng. **25**, 027002 (2015).
[32] D. Yuan, C. Pan, J. Zhang, S. Yan, Q. Zhao, G. Alici, and W. Li, Tunable particle focusing in a straight channel with symmetric semicircle obstacle arrays using electrophoresis-modified inertial effects, Micromachines **7**, 195 (2016).
[33] N. Cevheri and M. Yoda, Electrokinetically driven reversible banding of colloidal particles near the wall, Lab Chip **14**, 1391 (2014).
[34] N. Cevheri and M. Yoda, Lift forces on colloidal particles in combined electroosmotic and poiseuille flow, Langmuir **30**, 13771 (2014).
[35] J. Zheng and E. S. Yeung, Anomalous radial migration of single DNA molecules in capillary electrophoresis, Anal. Chem. **74**, 4536 (2002).
[36] J. Zheng and E. S. Yeung, Mechanism for the separation of large molecules based on radial migration in capillary electrophoresis, Anal. Chem. **75**, 3675 (2003).
[37] J. E. Butler, O. B. Usta, R. Kerkre, and A. J. C. Ladd, Kinetic theory of a confined polymer driven by an external force and pressure-driven flow, Phys. Fluids **19**, 113101 (2007).

[38] R. Kekre, J. E. Butler, and A. J. C. Ladd, Role of hydrodynamic interactions in the migration of polyelectrolytes driven by a pressure gradient and an electric field, Phys. Rev. E **82**, 050803 (2010).
[39] O. B. Usta, J. E. Butler, and A. J. C. Ladd, Transverse Migration of a Confined Polymer Driven by an External Force, Phys. Rev. Lett. **98**, 098301 (2007).
[40] M. Arca, J. E. Butler, and A. J. C. Ladd, Transverse migration of polyelectrolytes in microfluidic channels induced by combined shear and electric fields, Soft Matter **11**, 4375 (2015).
[41] M. Arca, A. J. C. Ladd, and J. E. Butler, Electro-hydrodynamic concentration of genomic length DNA, Soft Matter **12**, 6975 (2016).
[42] L. Rems, D. Kawale, L. J. Lee, and P. E. Boukany, Flow of DNA in micro/nanofluidics: From fundamentals to applications, Biomicrofluid. **10**, 043403 (2016).
[43] C. Liu and G. Hu, High-throughput particle manipulation based on hydrodynamic effects in microchannels, Micromachines **8**, 73 (2017).
[44] R. Vishnampet and D. Saintillan, Concentration instability of sedimenting spheres in a second-order fluid, Phys. Fluids **24**, 073302 (2012).
[45] J. Einarsson and B. Mehlig, Spherical particle sedimenting in weakly viscoelastic shear flow, Phys. Rev. Fluids **2**, 063301 (2017).
[46] D. Li, X. Lu, J. Wang, D. Li, and X. Xuan, Sheathless electrokinetic particle separation in a bifurcating microchannel, Biomicrofluid. **10**, 054104 (2016).
[47] J. Einarsson, M. Yang, and E. S. G. Shaqfeh, Einstein viscosity with fluid elasticity, Phys. Rev. Fluids **3**, 013301 (2018).
[48] J. Horvath and V. Dolnik. Polymer wall coatings for capillary electrophoresis, Electrophor. **22**, 644 (2001).
[49] X. Xuan, Joule heating in electrokinetic flow, Electrophor. **29**, 33 (2008).
[50] D. Di Carlo, Inertial microfluidics, Lab Chip **9**, 3038 (2009).
[51] X. Lu and X. Xuan, Elasto-inertial pinched flow fractionation for continuous shape-based particle separation, Anal. Chem. **87**, 11523 (2015).
[52] E. Yariv, Force-free electrophoresis?, Phys. Fluids **18**, 031702 (2006).
[53] L. Liang, Y. Ai, J. Zhu, S. Qian, and X. Xuan, Wall-induced lateral migration in particle electrophoresis through a rectangular microchannel, J. Colloid Interface Sci. **347**, 142 (2010).
[54] E. Yariv, Dielectrophoretic sphere–wall repulsion due to a uniform electric field, Soft Matter **12**, 6277 (2016).
[55] Z. Liu, D. Li, Y. Song, X. Pan, D. Li, and X. Xuan, Surface-conduction enhanced dielectrophoretic-like particle migration in electric-field driven fluid flow through a straight rectangular microchannel, Phys. Fluids **29**, 102001 (2017).
[56] L. G. Leal, The motion of small particles in non-Newtonian fluids, J. Non-Newton. Fluid Mech. **5**, 33 (1979).
[57] A. M. Leshansky, A. Bransky, N. Korin, and U. Dinnar, Tunable Nonlinear Viscoelastic Focusing in a Microfluidic Device, Phys. Rev. Lett. **98**, 234501 (2007).
[58] X. Lu, S. Patel, M. Zhang, S. Joo, S. Qian, A. Ogale, and X. Xuan, An unexpected particle oscillation for electrophoresis in viscoelastic fluids through a microchannel constriction, Biomicrofluid. **8**, 021802 (2014).
[59] D. F. James, Boger fluids, Annu. Rev. Fluid Mech. **41**, 129 (2009).
[60] R. J. Hunter, *Zeta Potential in Colloid Science* (Academic Press, New York, 1981).
[61] J. Happel and H. Brenner, *Low Reynolds Number Hydrodynamics: with Special Applications to Particulate Media*, 2nd ed. (Prentice-Hall, Englewood Cliffs, 1973).
[62] L. E. Rodd, T. P. Scott, D. V. Boger, J. J. Cooper-White, and G. H. McKinely, The inertio-elastic planar entry flow of low-viscosity elastic fluids in micro-fabricated geometries, J. Non-Newton. Fluid Mech. **129**, 1 (2005).
[63] H. Ranchon, R. Malbec, V. Picot, A. Boutonnet, P. Terrapanich, P. Joseph, T. Leichle, and A. Bancaud, DNA separation and enrichment using electro-hydrodynamic bidirectional flows in viscoelastic liquids, Lab Chip **16**, 1243 (2016).
[64] L. Liang, S. Qian, and X. Xuan, Three-dimensional electrokinetic particle focusing in a rectangular microchannel, J. Colloid Interface Sci. **350**, 377 (2010).